Acta Cryst. (1998). D**54**, 1387–1394

Estimating Lysozyme Crystallization Growth Rates and Solubility from Isothermal Microcalorimetry

Patricia A. Darcy and John M. Wiencek*

Department of Chemical and Biochemical Engineering, The University of Iowa, Iowa City, IA 52242, USA. E-mail: john-wiencek@uiowa.edu

(*Received 23 January 1998; accepted 24 April 1998*)

Abstract

A microcalorimetric technique has been developed to measure crystal-growth kinetics and enthalpies of crystallization. The enthalpy of crystallization of hen egg-white lysozyme in 0.1 *M* acetate buffer at pH 4.6 was determined at 287 K using this technique. The enthalpies were directly measured to be -14.3 ± 2.0 and -14.6 ± 1.3 kcal mol^{-1} (1 kcal mol^{-1} = 4.184 kJ mol^{-1}) for 3 and 5% NaCl solutions, respectively, which is in good agreement with values estimated from previous solubility measurements. Non-linear regression of the transient heat flow allowed measurement of the crystal growth rate as a function of protein supersaturation as well as the solubility. The crystal growth rates determined by this method were found to agree with those in the literature under the same solution conditions.

1. Introduction

Knowledge of detailed protein structure is essential for a rational approach to protein engineering and has important implications for the design of improved small-molecule pharmaceuticals. Production of high-quality protein crystals is required for molecular structure determination by X-ray crystallography.

Temperature provides a means of dynamically controlling rates of nucleation and growth. Predictive temperature-control strategies have been used in the past to control growth rates in inorganic crystallization processes (Jones & Mullin, 1974); however, such strategies have only recently been applied to protein crystallization. DeLucas and coworkers (Bray *et al.*, 1998), Ward *et al.* (1992) and Wiencek and coworkers (Schall, Riley *et al.*, 1996) have employed temperature control to protein crystallization in batch microdrop systems. DeLucas and Ward utilized active feedback (*i.e.* light scattering) to determine the onset of nucleation and then relied on scanning a variety of temperature profiles to arrive at an optimum temperature-control algorithm. Wiencek characterized key features of the system including critical nucleation temperatures, solubility and growth rates to arrive at a predetermined temperature-control algorithm. Both approaches benefit tremendously from an accurate knowledge of crystal-growth kinetics and the temperature dependence of the protein solubility.

To characterize protein crystallization, it is necessary to first obtain phase-diagram information. A phase diagram provides a method for quantifying the influence of solution parameters on the production of crystals (Saridakis *et al.*, 1994). A phase diagram, known as a Miers diagram, is shown in Fig. 1 for a protein displaying a typical temperature-dependent solubility. The diagram is divided into three regions: the stable zone, where the protein concentration is below the solubility concentration [(1) in Fig. 1]; the metastable zone, where the concentration of protein in solution is greater than the solubility concentration and growth of existing crystals occurs [(2) in Fig. 1]; and the labile zone, where the concentration of protein in solution is much greater than the solubility concentration and spontaneous nucleation as well as crystal growth occurs [(3) in Fig. 1]. To obtain large crystals with minimal nucleation, one temperature-control strategy would be to reduce the protein-solution temperature and enter the labile zone to allow nucleation. After a short time, the temperature would be elevated and the solution placed into the metastable zone to halt the nucleation and allow crystal growth. The crystal growth could then be controlled by decreasing the temperature at a predetermined rate in order to maintain a constant growth rate as recommended by Wiencek (Schall, Riley *et al.*, 1996). This requires knowledge of both crystal-growth kinetics and of the solubility as a function of temperature.

Solubility curves have traditionally been determined by either crystallization of a supersaturated solution or by dissolution of crystals in an undersaturated solution at several temperatures. Crystallization conditions must be known in advance for both methods. The main disadvantages of these methods for solubility determination are the amount of protein required (typically gram quantities) and the time (6–12 weeks) required. The protein may be recovered at the end of the experiment if contamination has not occurred. Cacioppo *et al.* (1991) have developed a micro-method for protein solubility determinations. This method requires about 200 mg of protein or less to determine key regions of a

ISSN 0907-4449

protein's solubility diagram. Broide and coworkers (Broide *et al.*, 1996; Berland *et al.*, 1992) measured solid–liquid phase boundaries for protein solutions by alternate heating and cooling of a crystal. The dissolving temperature is the minimum temperature at which the sharp edges of the crystal are rounded.

Crystal-growth rates are typically measured by video microscopy. A standard configuration consists of a light microscope with some form of temperature control of the optical stage where the crystals are observed. A video camera and time-lapse recorder are often used to obtain images of the crystals over a period of time (Durbin & Feher, 1986). Images can also be captured by a computer in a time-dependent manner for subsequent analysis using image-analysis software. Pusey (1994) has developed a computer-controlled apparatus able to simultaneously follow the growth rate of up to 40 crystals. Typical experiments may require a week or more for growth-rate analysis at a fixed solution condition and temperature.

Microcalorimetry has the potential to be a useful tool for determining: (i) the metastable–labile zone boundary, (ii) the temperature-dependence of protein solubility in a given solvent and (iii) the crystal-growth rates as a function of supersaturation. Microcalorimeters can detect a power signal as low as a few microwatts whereas standard calorimeters detect signals in the milliwatt range. Because of this greater sensitivity, samples with small heat effects, such as a crystallizing protein, can be analyzed.

The use of microcalorimetry in protein crystallization has been limited to the determination of the enthalpy of crystal formation, ΔH_{cry}, for lysozyme. Takizawa & Hayashi (1976) measured ΔH_{cry} of a 20 ml lysozyme solution in 3% NaCl adjusted to a pH of 4.2, at 288 K in a twin microcalorimeter. They reported a value of ΔH_{cry} of -25.1 ± 5.0 kcal mol^{-1}. Wiencek and coworkers (Schall, Arnold *et al.*, 1996) have also reported ΔH_{cry} for two lysozyme solutions (5% NaCl, final pH 4.6 at 288 K and 3% NaCl, final pH 5.2 at 288 K). Exact comparisons between these calorimetrically determined values of ΔH_{cry} and that of Takizawa & Hayashi could not be made since the buffer conditions were not identical. Wiencek and coworkers (Schall, Arnold *et al.*, 1996) compared their enthalpies to those obtained from a van't Hoff plot of solubility *versus* temperature under the same conditions. The van't Hoff values of -15.1 ± 1.3 kcal mol^{-1} (5% NaCl) and -8.1 ± 2.7 kcal mol^{-1} (3%) were in agreement with the calorimetrically determined values of -17.1 ± 3.2 and -10.5 ± 2.3 kcal mol^{-1}.

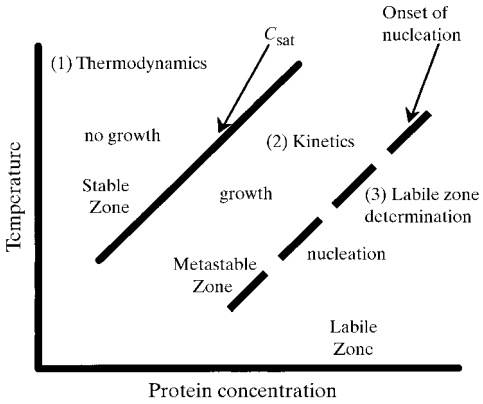

Fig. 1. A Miers diagram for a typical protein. Three regions of nucleation/growth behavior are shown. The first region is the stable zone where the protein remains in solution. The second region is the metastable zone where the solution is supersaturated and growth of existing crystals occurs but nucleation is minimal. The third region is the labile zone where the solution is at a high enough supersaturation for spontaneous nucleation, as well as growth, to occur.

In these previous studies, microcalorimetry has been used to determine enthalpies of crystallization only. Protein-crystallization kinetics and solubilities were not determined calorimetrically. The present work is concerned with the analysis of the transient heat signal to yield crystal-growth kinetics and solubility information. The typical calorimetry experiment takes only two or three days and milligrams of protein *versus* weeks or months and grams of protein for classical methods of solubility and growth-rate determination. This paper addresses the calorimetric determination of crystal-growth rates and solubility as a function of temperature for lysozyme.

2. Materials and methods

2.1. *Sample preparation and data collection*

Hen egg-white lysozyme was purchased from Sigma Chemicals (L-6876, lot 65H7025). The lysozyme solutions were prepared by dialysis at 277 K over 2 d against deionized water, then against 0.1 *M* acetate buffer pH 4.6 using a 3500 molecular-weight cut-off membrane (Spectra/Por). Stock solutions of lysozyme were concentrated using a 10000 molecular-weight cut-off concentrator (Amicon). Stock solutions of 10 and 15% NaCl were prepared in 0.1 *M* acetate buffer pH 4.6. All solution concentrations reported as percentages are percent weight per volume, %(*w*/*v*). All buffers were prepared by making two solutions, 0.1 *M* sodium acetate and 0.1 *M* acetic acid, and mixing the two solutions to obtain the desired pH of 4.6. Protein stock solutions were mixed with appropriate volumes of acetate buffer and NaCl stock solutions to obtain the desired final protein and NaCl concentrations. Lysozyme concentrations were determined using an extinction coefficient of 26.35 for a 10 mg ml^{-1} solution at 280 nm (Sophianopoulos *et al.*, 1962). All stock solutions were passed through a 0.2 µm syringe filter before sample preparation.

The heat signal from a crystallizing solution of lysozyme was recorded using a differential-scanning calori-

meter (DSC) model 4110 manufactured by CSC Co. (Provo, UT). The reference cell and three sample cells were 1 ml capacity Hastelloy screw-top ampoules with gaskets. To determine the enthalpy of crystallization, the calorimeter was operated in an isothermal mode. In this mode, the calorimeter recorded power, in microwatts, *versus* time.

Baselines were determined for each cell before the crystallization runs. 1 ml of 3% NaCl in 0.1 *M* acetate buffer was placed in each cell and the sample weights (approximately 1 g) were recorded. The reference cell was placed in the calorimeter at room temperature and the DSC was cooled to the desired value of 287 K. After the system reached and maintained this temperature, the three sample cells were placed in the calorimeter and the heat signal collected every minute for 7 h. At the end of the run, the three sample cells were removed, but the reference cell was left in the calorimeter for subsequent baseline or sample runs.

For the lysozyme-sample runs, a 4 ml sample of the desired lysozyme and NaCl concentration was prepared, approximately 1 ml was placed in each of the three sample cells and the sample weights were recorded. Glass cover slips were cut into approximately 0.5 × 0.5 mm squares using a diamond-tip pencil. A glass square was carefully placed in each cell. Lysozyme crystals tended to stick to these glass squares and allowed for crystal size determination at the end of the experiments. When the system temperature reached 287 K, the sample cells (now containing the lysozyme solution) were placed in the calorimeter and the heat signal was collected every 1–2 min for 2–3 d. At the end of the run, the sample cells were removed while the system was still at 287 K to avoid any melting of the crystals. Final crystal sizes were determined by acquiring images of crystals on the walls of the cells, on the glass cover slips and floating in solution using a stereo microscope and video imaging analysis software (Mocha, Jandel Scientific). The final lysozyme concentrations were obtained by removing an aliquot of crystal-free solution and measuring the absorbance at 280 nm.

After every run, the cells were cleaned by sonicating for 10–15 min in several solutions in the following order: deionized water, methanol, deionized water, 1 *M* KOH and finally copious amounts of deionized water. This protocol ensured that the lysozyme was completely removed from the cells. The cells were then placed in a drying oven for several hours. The rubber gaskets were cleaned in a similar manner except the 1 *M* KOH was omitted and they were allowed to dry in air.

The solubility of lysozyme at 287 K in both 3 and 5% NaCl was determined by batch crystallization and dissolution experiments. The lysozyme was prepared as described above and held isothermally at 287 K. Ten 1.0 ml samples at each NaCl concentration under both dissolving and crystallizing conditions were periodically sampled for liquid-phase lysozyme concentration (*i.e.* a total of 40 samples). The average and standard deviation of the liquid-phase lysozyme concentration were used to determine the solubility as described below.

2.2. *Data analysis*

Raw power *versus* time curves, for baseline and sample runs, were normalized by dividing the power signal by the sample weight. For each cell, seven baseline runs were obtained. Data was collected for 7 h after the cells were placed in the calorimeter. Allowing for thermal equilibration, data collected for the first 90 min after the cells were placed in the calorimeter were omitted and the time adjusted to zero. The average value of the last 15 min of each baseline run was subtracted from the data set. This was to normalize the data sets to approach zero at the end of each run and allow the use of a single decaying exponential function without regressing a superfluous baseline value (Fig. 2). These baseline functions were subtracted from the normalized sample runs to give the power *versus* time data sets to be analyzed (Fig. 3).

An Excel spreadsheet incorporating material balances and a crystal growth rate expression is used to model the power signal using a finite-difference method. The model parameters are the empirical growth-rate parameters k and n, the solubility C_{sat}, the baseline P_{bl} and the induction time t_{nuc}. Note that C_{sat} is in mg ml^{-1}, P_{bl} is in μW, t_{nuc} is in s and k has units of μm min^{-1} mg^{-n} ml^{n}. At $t = 0$, the concentration of protein in solution is $C(0) = C_0$ and the number of moles of protein in the crystals is $M(0) = 0$. ΔH_{cry} is calculated by summing the area under the power *versus* time curve and dividing by the total moles of lysozyme incorporated into the crystalline state, M_f (equation 1). The number of moles of crystalline lysozyme at the end of the experiment is calculated by multiplying the difference between the initial and final lysozyme concentra-

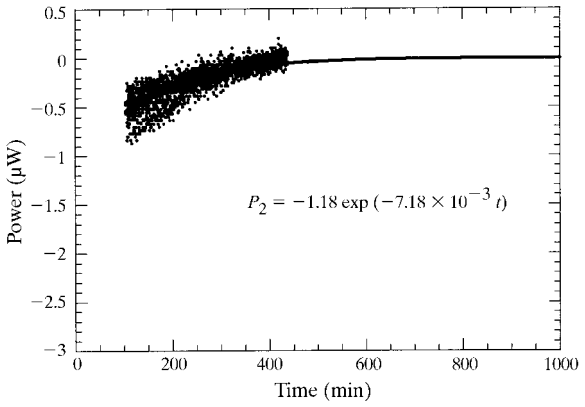

Fig. 2. Power *versus* time for seven baseline runs in a typical cell. ●, calorimetry data; unbroken line, model fit. The seven data sets were fitted to an exponential, $P = -1.18 \exp(-7.18 \times 10^{-3} t)$.

tions in solution, C_o and C_f, by the volume of solution $V_{\rm sol}$ and dividing by the molecular weight of lysozyme (M_w = 14400).

$$\Delta H_{\rm cry} = \frac{1}{M_f}\int_0^{t_f}(P_{\rm raw} - P_{\rm bl})\mathrm{d}t = \left[\frac{M_w}{V_{\rm sol}(C_o - C_f)}\right]\int_0^{t_f}(P_{\rm raw} - P_{\rm bl})\mathrm{d}t. \quad (1)$$

The number of moles of crystalline lysozyme at any instant in time, $M(t)$, is calculated by dividing the instantaneous heat, $Q(t)$, by $\Delta H_{\rm cry}$,

$$M(t) = \left(\int_0^t P\mathrm{d}t\right)/\Delta H_{\rm cry} = Q(t)/\Delta H_{\rm cry}. \quad (2)$$

The crystal-face-growth rate, G, in μm min^{-1}, is calculated using an empirical power-law expression with parameters k and n and the protein solubility $C_{\rm sat}$,

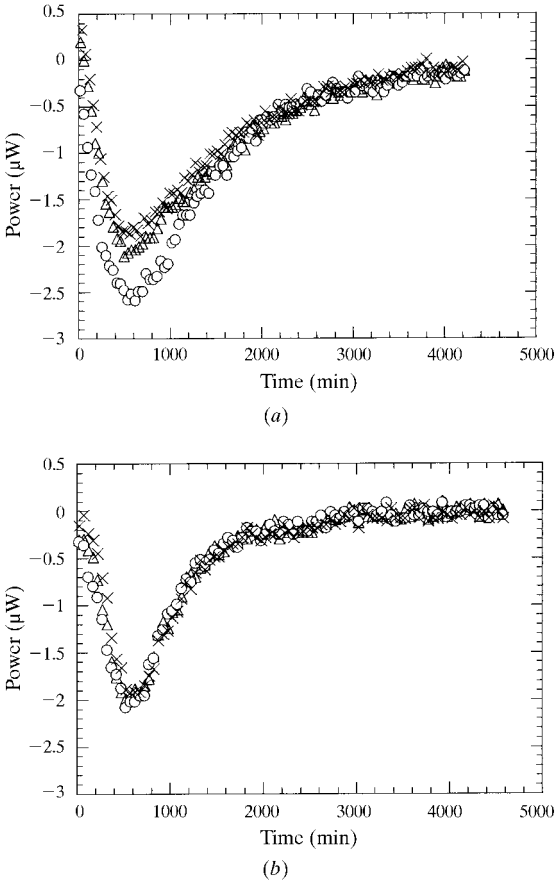

Fig. 3. The measured signals from the microcalorimeter for two sets of crystallizing solutions of lysozyme, 0.1 *M* acetate buffer pH 4.6 at 287 K. △, sample one; ○, sample two; ×, sample three. To distinguish the three data sets, only 5% of the total data is displayed. (*a*) Initial lysozyme concentration of 64.3 mg ml^{-1} in 3% NaCl solution. (*b*) Initial lysozyme concentration of 31.5 mg ml^{-1} in 5% NaCl solution.

$$G(t) = \frac{\mathrm{d}L}{\mathrm{d}t} = k[C(t) - C_{\rm sat}]^n. \quad (3)$$

The characteristic length, $L(t)$, typically given in μm, is calculated as a function of time *via* a finite-difference approximation of the definition of G,

$$L(t + \Delta t) = L(t) + G(t)\Delta t. \quad (4)$$

The number of moles of crystalline lysozyme is proportional to the volume of the crystal which, in turn, is proportional to the cube of the characteristic length provided the aspect ratio (*i.e.* relative face-growth rates) remains constant during growth,

$$M(t)/M_f = L(t)^3/L_f^3. \quad (5a)$$

Thus, the change in the number of crystalline lysozyme moles with respect to time can be calculated,

$$\frac{\mathrm{d}M}{\mathrm{d}t}(t) = 3\frac{M_f}{L_f^3}L(t)^2\frac{\mathrm{d}L}{\mathrm{d}t} = 3\frac{M_f}{L_f^3}L(t)^2G(t). \quad (5b)$$

A mole balance on the protein (in the liquid and the crystals) gives the concentration of protein in solution as a function of time, $C(t)$,

$$C(t + \Delta t) = C(t) - \frac{M_w}{V_{\rm sol}}\frac{\mathrm{d}M}{\mathrm{d}t}(t)\Delta t. \quad (6)$$

The model power signal is calculated by adding a baseline value to the power signal,

$$P_{\rm model}(t) = P_{\rm bl} + \Delta H_{\rm cry}\frac{\mathrm{d}M}{\mathrm{d}t}(t). \quad (7)$$

The error between this model power and the calorimeter power data is minimized by adjusting the baseline value ($P_{\rm bl}$), the solubility ($C_{\rm sat}$) and the growth-rate parameters (k and n). The induction time (onset of nucleation, $t_{\rm nuc}$) is separately adjusted until a minimum in the error is obtained.

$\Delta H_{\rm cry}$ and $C_{\rm sat}$ at one temperature (T_1) are used to calculate the solubility as a function of temperature *via* the van't Hoff equation (b is calculated from the known data pair of $C_{\rm sat}$ and T_1),

$$\ln C_{\rm sat} = (\Delta H_{\rm cry}/R)[(1/T) - b]. \quad (8)$$

The results of the model regression yields $\Delta H_{\rm cry}$ and $C_{\rm sat}$ at the temperature of the experiment; thus, the entire temperature–solubility curve can be calculated from this one experiment.

3. Results and discussion

Power *versus* time signals for three lysozyme sample runs in 3 and 5% NaCl are shown in Fig. 3. The three data sets in 3% NaCl do not completely overlap. Sample two has a peak heat flow of −2.5 μW compared with samples one and three which have a peak of approximately −2.0 μW. This observation is consistent with increased nucleation in sample two. The number of

Table 1. *Summary of lysozyme crystallization runs.*

Conditions: 0.1 *M* acetate buffer pH 4.6, 287 K. The initial and final protein concentrations, C_o and C_f, are measured *via* UV/vis spectroscopy. ΔH_{cry} is determined calorimetrically and the solubility and crystal-growth-rate parameters, k and n, are determined *via* non-linear regression of the calorimetry data. Literature values are from regressed data (Cacioppo & Pusey, 1991).

(*a*) 3% NaCl.

C_o (mg ml^{-1})	C_f (mg ml^{-1})	k (μm min^{-1} mg^{-n} ml^n)	n	C_{sat} (287 K) (mg ml^{-1})	ΔH_{cry} (kcal mol^{-1})
58.6	18.9	1×10^{-6}	3.3	6.4	−13.6
58.6	18.6	7×10^{-7}	3.4	6.3	−11.2
59.1	15.6	4×10^{-7}	3.4	0	−13.8
59.1	16.0	4×10^{-6}	2.9	4.3	−15.9
64.3	17.6	9×10^{-7}	3.2	0	−14.9
64.3	16.8	8×10^{-6}	2.7	6.0	−17.3
64.3	18.5	7×10^{-6}	2.8	5.0	−13.4
Mean standard deviation		$3 \times 10^{-6} \pm 3 \times 10^{-6}$	3.1 ± 0.3	4.0 ± 2.8	−14.3 ± 2.0
Literature value				4.4 ± 1.1	−15.5 ± 0.3

(*b*) 5% NaCl.

C_o (mg ml^{-1})	C_f (mg ml^{-1})	k (μm min^{-1} mg^{-n} ml^n)	n	C_{sat} (287 K) (mg ml^{-1})	ΔH_{cry} (kcal mol^{-1})
42.1	3.9	5×10^{-3}	1.2	3.9	−13.2
42.1	4.4	4×10^{-3}	1.4	4.3	−12.4
31.5	4.2	4×10^{-3}	1.5	3.7	−15.1
31.5	4.3	6×10^{-3}	1.4	4.0	−15.2
31.5	4.4	2×10^{-3}	1.7	3.4	−14.9
35.3	3.8	3×10^{-3}	1.4	3.4	−15.7
35.3	4.0	6×10^{-3}	1.3	3.9	−15.8
Mean standard deviation		$4 \times 10^{-3} \pm 1 \times 10^{-3}$	1.4 ± 0.2	3.8 ± 0.3	−14.6 ± 1.3
Literature value				1.3 ± 1.1	−13.6 ± 0.5

crystals formed can be calculated from average final crystal length and the total mass of crystals formed. Sample two has twice the estimated number of crystals of either sample one or three. Nucleation is a random process. More crystals nucleating in sample two is seen as a sharper and larger power-signal peak as more heat is generated initially and more crystals continue to grow at the same rate. For the 5% NaCl run, the three samples have approximately the same number of crystals. In view of the equal number of crystals, these three data sets overlap as expected.

Some typical model power signals are compared to the experimental data in Fig. 4. For example, the regression of the particular 3% NaCl data set shown in Fig. 4(*a*) gives an estimate of 6.0 mg ml^{-1} for the lysozyme solubility at 287 K. Likewise, the growth-rate parameters, k and n, for this particular data set are 7.79×10^{-6} μm min^{-1} mg^{-n} ml^n and 2.72, respectively. Multiple data sets are used to arrive at average values and error estimates for C_{sat}, k and n.

Table 1 gives a summary of the enthalpies of crystallization and growth-rate parameters obtained for the two lysozyme solutions studied (3 and 5% NaCl, pH 4.6) from seven replications of the experiment. ΔH_{cry} for lysozyme at 287 K is -14.3 ± 2.0 kcal mol^{-1} for the 3% NaCl solution and -14.6 ± 1.3 kcal mol^{-1} for the 5% NaCl solution. Solubility data under comparable solution conditions over a temperature range of 277–298 K are available (Cacioppo & Pusey, 1991). The solubility is reported as a polynomial expansion in temperature. Such an expression is convenient for quickly calculating solubility at a given temperature, but fails to provide an adequate estimate of experimental error. In order to provide a meaningful comparison of his data with the current work, Dr Pusey graciously supplied the raw data utilized to derive the polynomials. A regression of this raw data to a van't Hoff equation yields the estimates for ΔH_{cry} and C_{sat} (287 K) shown in Table 1. The ΔH_{cry} of -14.3 kcal mol^{-1} obtained calorimetrically for the 3% NaCl solution is in agreement with the value of -15.5 kcal mol^{-1} extracted from the solubility data of Cacioppo & Pusey (1991). Likewise, the calorimetrically determined ΔH_{cry} value of -14.6 kcal mol^{-1} of the 5% NaCl solution agrees with the value of -13.6 kcal mol^{-1} from the solubility data of Cacioppo & Pusey (1991).

The solubility can be determined as a function of temperature *via* van't Hoff analysis using the solubility at one temperature (287 K in this case) and the ΔH_{cry} value determined calorimetrically. Fig. 5 shows a van't Hoff plot of the calorimetrically determined solubility as a function of temperature for the 3% NaCl solution. The solid line is calculated using the average values for ΔH_{cry} and C_{sat}, whereas the dotted lines indicate the upper and lower bounds based on the propagation of error using the variance in both ΔH_{cry} and C_{sat} as independent error estimates for these parameters.

Pusey's raw solubility data under the same conditions are shown for comparison. The calorimetrically determined solubility data agrees quite well with the literature values for this solution condition. In a similar fashion, Fig. 6 shows the calorimetrically determined solubility data for the 5% NaCl solution. Pusey's solubility data under the same conditions are again shown for comparison. The calorimetrically determined solubilities are higher then those obtained by Pusey. Many explanations can be postulated for the disagreement. An obvious explanation is that the data analysis provides an estimate of the concentration at which the growth rate becomes zero, which is assumed to equal the solubility. However, Monaco & Rosenberger (1993) found that a 'dead zone' exists at a relative supersaturation [*i.e.* $(C - C_{sat})/C_{sat}$] of 2.0, below which growth ceased. Vekilov *et al.* (1995) confirmed the existence of this dead zone in a separate study, albeit at a lower range of relative supersaturation (1.5). The reduced dead-zone width was attributed to the more purified protein solution used in Vekilov's study. The current study uses lysozyme that is similar to the lysozyme used by Monaco & Rosenberger (1993). Assuming the true solubility to be 1.09 mg ml^{-1}, as reported by Cacioppo & Pusey (1991), and that the lysozyme in the calorimeter did stop growing upon encountering this dead zone, the dead zone can be calculated to be encountered at a relative supersaturation of 2.47 $\pm$ 0.29. This value agrees with the range reported by Monaco & Rosenberger (1993). The apparent absence of such a 'dead zone' effect in the 3% NaCl data may be attributed to the much larger variation in the regressed values of C_{sat}. In any case, it is evident that estimates of solubility from a solution which is crystallizing will always yield results which are larger than the true solubility owing to the long times required to attain equilibrium. Extrapolation to zero growth, as

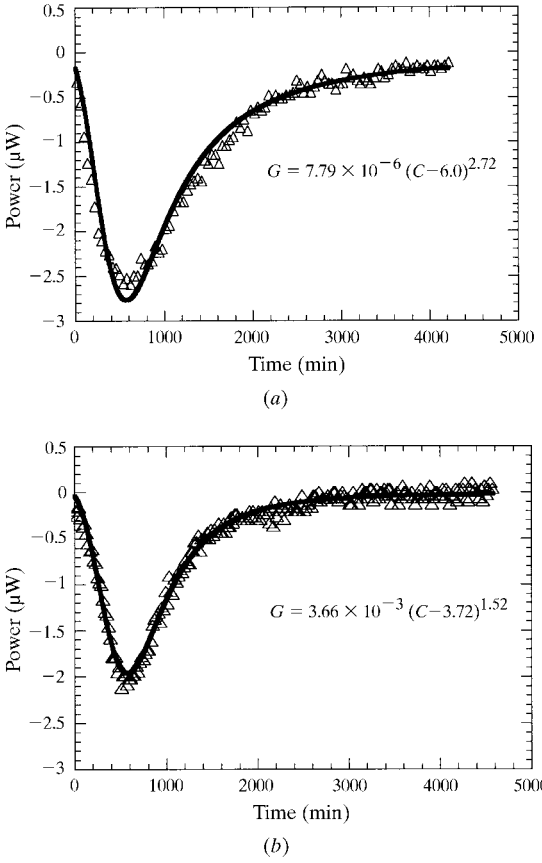

Fig. 4. The measured signal of a lysozyme solution, 0.1 *M* acetate buffer pH 4.6 at 287 K. 5% of the total data is displayed. The calorimeter data was fitted to a model using a power-law growth rate for the crystal growth, $G = k(C - C_{sat})^n$. △, calorimetry data; unbroken line, model fit. (*a*) Initial lysozyme concentration of 64.3 mg ml^{-1} in 3% NaCl solution, with C_{sat} = 6.0 mg ml^{-1}, k = 7.79 × 10^{-6} μm min^{-1} mg^{-n} ml^n and n = 2.72. (*b*) Initial lysozyme concentration of 31.5 mg ml^{-1} in 5% NaCl solution, with C_{sat} = 3.72 mg ml^{-1}, k = 3.66 × 10^{-3} μm min^{-1} mg^{-n} ml^n and n = 1.52.

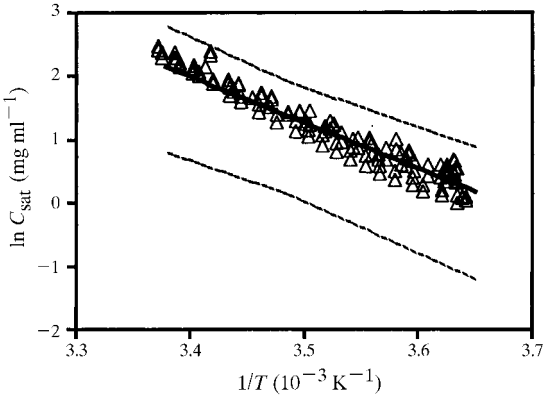

Fig. 5. van't Hoff plot of lysozyme solubility in 0.1 *M* acetate buffer pH 4.6, 3% NaCl, as a function of temperature. △, Pusey's solubility data; unbroken line, solubility calculated by using the ΔH_{cry} and C_{sat} determined calorimetrically at 287 K; dashed line, solubility range encompassed by propagation-of-error estimates for ΔH_{cry} and C_{sat}.

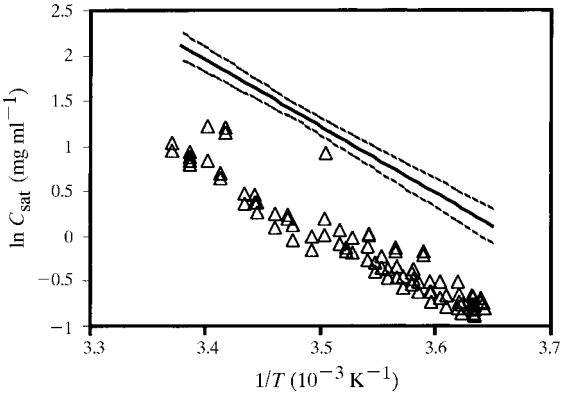

Fig. 6. van't Hoff plot of lysozyme solubility in 0.1 *M* acetate buffer pH 4.6, 5% NaCl, as a function of temperature. △, Pusey's solubility data; unbroken line, solubility calculated by using the ΔH_{cry} and C_{sat} determined calorimetrically at 287 K; broken line, solubility range encompassed by propagation-of-error estimates for ΔH_{cry} and C_{sat}.

performed above, will not always yield a true solubility if a growth dead zone exists.

To further verify the existence of the dead zone in this lysozyme system, the concentration of lysozyme in the liquid phase was measured in samples of both growing and dissolving lysozyme crystals. Both the 3 and 5% NaCl systems show a nonconvergence of the crystallizing and dissolving systems (see Fig. 7). Traditionally, one would take the average of the two values and the difference would be an estimate of the error. However, it is more likely that the dissolving crystals yield the more accurate value since the dissolution process does not display the dead-zone phenomena seen in the growing lysozyme-crystal system. The values of the dissolving experiments are much closer to the values reported by Cacioppo & Pusey (1991).

This result suggests an effective strategy for obtaining accurate temperature–solubility data. The calorimetric experiment is run and interpreted as discussed above. The resulting solubility estimates may be biased high, but will be more than adequate for most applications of temperature-controlled protein-crystal growth. If more accurate temperature–solubility data is required, the crystals from the calorimetry experiment can be harvested and fresh buffer added to them in order to carry out the dissolving solubility study. Dissolution is complete within two weeks and the resulting solubility value can be combined with ΔH_{cry} to yield an accurate

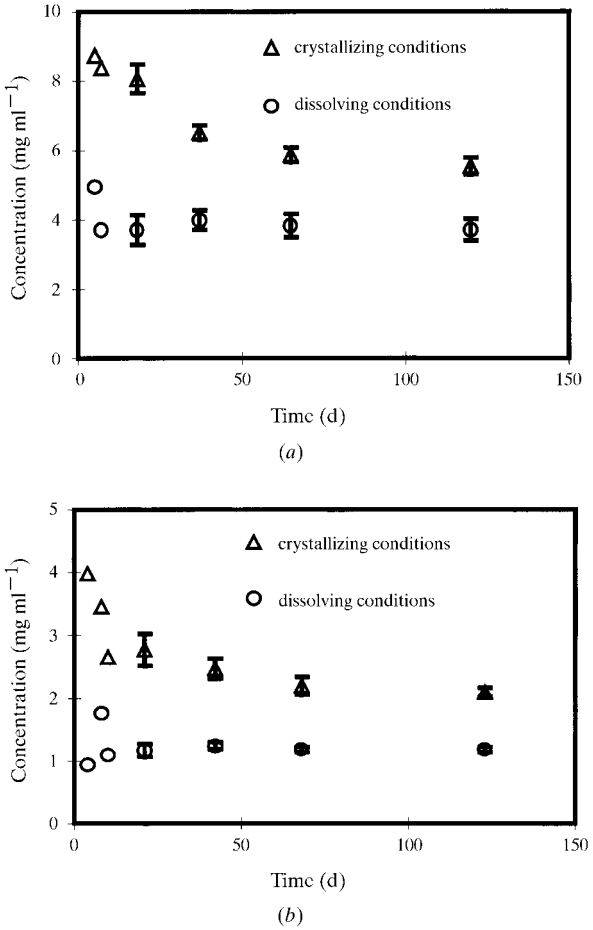

Fig. 7. Lysozyme liquid-phase concentration as a function of time in crystallizing as well as dissolving conditions. Average values of ten separate samples are reported with error bars of one standard deviation. The first two data points in the 3% data series and the first three data points in the 5% data series were single-point measurements; thus, no error bars are reported. (*a*) 3% NaCl at 287 K, asymptotic crystallizing solubility is 5.53 mg ml^{-1} (initial concentration of 49 mg ml^{-1}) and asymptotic dissolving solubility is 3.71 mg ml^{-1} (initial concentration of 0 mg ml^{-1}); (*b*) 5% NaCl at 287 K, asymptotic crystallizing solubility is 2.10 mg ml^{-1} (initial concentration of 36 mg ml^{-1}) and asymptotic dissolving solubility is 1.18 mg ml^{-1} (initial concentration of 0 mg ml^{-1}).

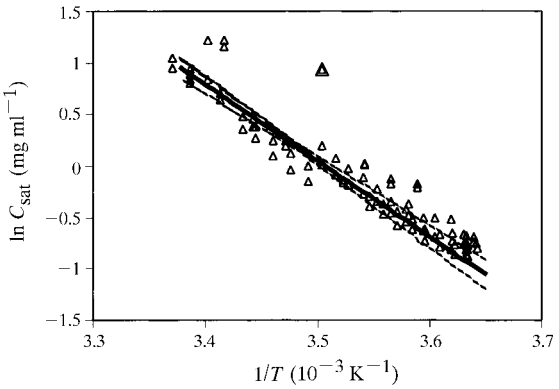

Fig. 8. Unbroken line, van't Hoff plot of lysozyme solubility utilizing dissolving solubility measurement from Fig. 7(*b*) and ΔH_{cry} determined calorimetrically. Solution conditions are 0.1 *M* acetate buffer pH 4.6 and 5% NaCl. △, Pusey's solubility data (for comparison) for same solution conditions. Dashed line, propagation of error in ΔH_{cry} and solubility at 287 K.

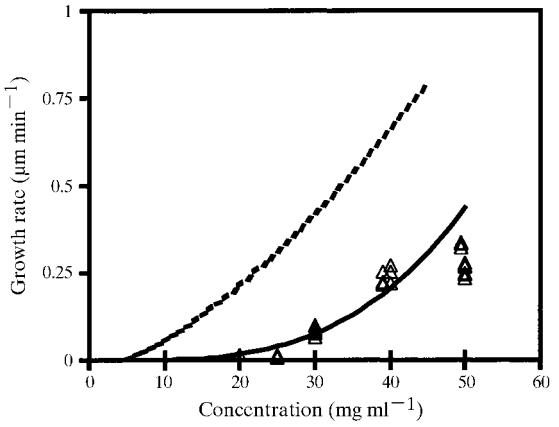

Fig. 9. Comparison of calorimetrically determined growth rates for lysozyme and Pusey's growth rate. 0.1 *M* acetate buffer at 287 K. △, Pusey's growth rate (Nadarajah *et al.*, 1995) in 3% NaCl solution; unbroken line, calorimetrically determined growth rate in 3% NaCl solution; broken line, calorimetrically determined growth rate in 5% NaCl solution.

temperature–solubility diagram. For example, the dissolving solubility for the 5% NaCl sample of 1.18 mg ml^{-1} (data from Fig. 7*b*) is combined with the previously measured ΔH_{cry} of -14.61 kcal mol^{-1} to yield a more accurate temperature–solubility diagram as shown in Fig. 8. This improved solubility line clearly fits Pusey's data.

Growth-rate data is available for direct comparison with calorimetrically determined growth rates for the 3% NaCl solution but not for the 5% NaCl solution. Fig. 9 shows a comparison of Pusey's growth rates (Nadarajah *et al.*, 1995) and the calorimetrically determined growth rates at 3 and 5% NaCl. The 3% NaCl data is in agreement with literature values obtained by microscopy methods. As expected, the 5% NaCl growth rates are higher than the 3% NaCl growth rates. For a given protein concentration, the 5% NaCl solution has a higher supersaturation compared to the 3% NaCl solution, owing to the reduced solubility of lysozyme at higher electrolyte concentrations. This higher supersaturation translates into a higher growth rate.

4. Conclusions

Obtaining large high-quality crystals is vital for high-resolution X-ray diffraction analysis. Dynamic temperature-control techniques used to control crystal nucleation and growth require knowledge of protein temperature–solubility diagrams as well as crystal-growth rates. Microcalorimetry provides accurate estimates of crystal-growth rates when compared with values obtained by standard techniques. The temperature–solubility diagram can also be extracted from the microcalorimetric data, but may provide solubility estimates which are biased to values larger than anticipated owing to dead zones in the growth curve. Even such data of reduced accuracy is of tremendous benefit when implementing temperature-controlled protein-crystal growth. If data of the highest accuracy is required, the calorimetric measurements can be supplemented with an isothermal dissolving solubility measurement to yield the temperature–solubility diagram. Microcalorimetry has the advantage of being fast, non-destructive to the protein and requiring a relatively small amount of material. One calorimetry run lasting two to three days and requiring a few milligrams of material can yield results which typically take months and grams of protein to obtain by standard techniques.

The authors would like to thank Dr Marc Pusey for the generous use of his solubility and growth-rate data. PAD was supported by a NASA GSRP fellowship. This work was funded by NASA Microgravity Science and Applications Division.

References

Berland, C. R., Thurston, G. M., Kondo, M., Broide, M. L., Pande, J., Ogun, O. & Bendek, G. B. (1992). *Proc. Natl Acad. Sci. USA*, **89**, 1214–1218.

Bray, T. L., Kim, L. J., Askew, R. P., Harrington, M. D., Rosenblum, W. M., Wilson, W. W. & DeLucas, L. J. (1998). *J. Appl. Cryst.* **31**(4), 515–522.

Broide, M. L., Tomine, T. M. & Saxowsky, M. D. (1996). *Phys. Rev. E*, **53**, 6325–6335.

Cacioppo, E., Munson, S. & Pusey, M. L. (1991). *J. Cryst. Growth*, **110**, 66–71.

Cacioppo, E. & Pusey, M. L. (1991). *J. Cryst. Growth*, **114**, 286–292.

DeLucas, L. J., Long, M. M., Moore, K. M., Smith, C., Carson, M., Narayana, S. V. L., Carter, D., Clark, A. D., Nanni, J., Ding, J., Jacobo-Molina, A., Kamer, Hughes, S. H., Arnold, E., Einspahr, H. M., Clancy, L. L., Rao, G. S. J., Cook, P. F., Harris, B. G., Munson, S. H., Finzel, B. C., McPherson, A., Weber, P. C., Lewandowski, F., Nagabhushan, T. L., Trotta, P. P., Reichert, P., Navia, M. A., Wilson, K. P., Thompson, J. A., Meade, C., Bishop, S. P., Dunbar, B. J., Trinh, E., Prahl, J., Sacco, A. & Bugg, C. E. (1994). *J. Cryst. Growth*, **135**, 183–195.

Durbin, S. & Feher, G. (1986). *J. Cryst. Growth*, **76**, 583–592.

Jones, A. G. & Mullin, J. W. (1974). *Chem. Eng. Sci.* **29**, 105–118.

Monaco, L. A. & Rosenberger, F. (1993). *J. Cryst. Growth*, **129**, 465–484.

Nadarajah, A., Forsythe, E. L. & Pusey, M. L. (1995). *J. Cryst. Growth*, **151**, 163–172.

Pusey, M. L. (1994). *Rev. Sci. Instrum.* **64**, 3121–3125.

Saridakis, E., Stewart, P., Lloyd, L. & Blow, D. (1994). *Acta Cryst.* D**50**, 293–297.

Schall, C. A., Arnold, E. & Wiencek, J. M. (1996). *J. Cryst. Growth*, **165**, 293–298.

Schall, C. A., Riley, J. S., Li, E., Arnold, E. & Wiencek, J. M. (1996). *J. Cryst. Growth*, **165**, 299–307.

Sophianopoulos, A. J., Rhodes, C. K., Holocomb, D. W. & Van Holde, K. E. (1962). *J. Biol. Chem.* **237**, 1107–1112.

Takizawa, T. & Hayashi, S. (1976). *J. Phys. Soc. Jpn*, **40**, 299–300.

Vekilov, P. G., Ataka, M. & Katsura, T. (1995). *Acta Cryst.* D**51**, 207–219.

Ward, K. B., Zuk, W. M., Perozzo, M. A., Walker, M. A., Birnbaum, G. I., Kung, W., Cavaliere, A., Uffen, D. R. & Scholaert, H. (1992). *J. Cryst. Growth*, **122**, 235–241.